ELSEVIER

Earth and Planetary Science Letters 172 (1999) 11–21

EPSL

www.elsevier.com/locate/epsl

Self-driven mode switching of earthquake activity on a fault system

Yehuda Ben-Zion [a,*], Karin Dahmen [b], Vladimir Lyakhovsky [c], Deniz Ertas [d], Amotz Agnon [e]

[a] *Department of Earth Sciences, Univ. of Southern CA, Los Angeles, CA 90089-0740, USA*
[b] *Department of Physics, University of Illinois at Urbana Champaign, 1110 West Green Street, Urbana, IL 61801-3080, USA*
[c] *Institute of Earth Sciences, The Hebrew University, Jerusalem, Israel*
[d] *Exxon Corporate Research Lab, Annandale, NJ 08801, USA*
[e] *Institute of Earth Sciences, The Hebrew University, Jerusalem, Israel*

Received 2 March 1999; revised version received 15 July 1999; accepted 29 July 1999

Abstract

Theoretical results based on two different modeling approaches indicate that the seismic response of a fault system to steady tectonic loading can exhibit persisting fluctuations in the form of self-driven switching of the response back and forth between two distinct modes of activity. The first mode is associated with clusters of intense seismic activity including the largest possible earthquakes in the system and frequency–size event statistics compatible with the characteristic earthquake distribution. The second mode is characterized by relatively low moment release consisting only of small and intermediate size earthquakes and frequency–size event statistics following a truncated power law. The average duration of each activity mode scales with the time interval of a large earthquake cycle in the system. The results are compatible with various long geologic, paleoseismic, and historical records. The mode switching phenomenon may also exist in responses of other systems with many degrees of freedom and nonlinear dynamics.

Keywords: earthquakes; dynamic properties; non-linear distortion; seismicity

1. Introduction

Seismicity patterns are characterized by a variety of fluctuations including foreshocks, aftershocks, periods of quiescence, migration of earthquakes along fault zones, switching of activity among different faults, and more [1]. It is, however, usually assumed that over time scales longer than a few large earthquake cycles and shorter than geological periods (e.g., 10^3 yr $\leq$ time $\leq 10^6$ yr in tectonically active areas), regional and local statistics of earthquakes are stationary in time. The most common types of statistics used to describe seismicity patterns of tectonic earthquakes are temporal decay of aftershock rates, and frequency–size distribution of earthquakes giving relative frequencies of events in different size ranges. It is widely accepted that, to first order, aftershock rates are distributed according to the modified Omori power law [2] regardless of location or time. In contrast, the form of frequency–size statistics is a much debated subject. Kagan [3–5] analyzed regional and global earthquake catalogs and argued, based on these observations, that frequency–size

* Corresponding author. Tel.: +1 213 740 6734; Fax: +1 213 740 8801; E-mail: benzion@terra.usc.edu

0012-821X/99/$ – see front matter
PII: S0012-821X(99)00187-9

statistics of tectonic earthquakes follow everywhere the Gutenberg–Richter power law relation with a roughly universal exponent (*b*-value close to 1). On the other hand, Wesnousky [6,7] and others [8,9] examined statistics of earthquakes in various individual fault systems occupying narrow and long spatial domains. The results emerging from the latter studies, and related theoretical works [10–12], suggest that Gutenberg–Richter type statistics in individual fault zones are limited to immature structures with strong geometric disorder. In contrast, frequency–size earthquake statistics in relatively regular structures, associated with highly slipped mature fault zones, are better described by a 'characteristic earthquake' distribution, consisting of power law statistics of small events combined with strong enhancement in the frequency of earthquakes having a certain 'preferred' size (see, e.g., the distribution at the bottom of region 2 in Fig. 5a).

In this paper we present theoretical results, based on two different modeling approaches [13,14], which show that in certain parameter ranges models of individual fault systems can switch spontaneously their mode of seismic response to slow tectonic loading, from a time interval with frequency–size statistics following the characteristic earthquake distribution to an interval with Gutenberg–Richter statistics and back. In the intervals associated with the characteristic earthquake distribution the largest possible events in the system occur, while in the periods associated with the Gutenberg–Richter statistics there are only small and intermediate size earthquakes. The activity switching results from episodic global reorganization of the mode of strain energy release in the system, associated with a statistical competition between a tendency for a synchronized behavior and a tendency for a disordered response. These tendencies are approximately equal for the range of model parameters generating mode switching of activity. The persistence time in each mode is scaled by the time of a large earthquake cycle on the generating fault system. Thus, the observation of mode switching in natural seismicity requires long records containing many large earthquake cycles. Although data sets of such long duration are not very common, available paleoseismic [15–22], historical [23,24], and geological [25,26] observations (see the Section 3) indicate that mode switching of seismic activity of the type simulated here may occur in nature. The mode switching phenomenon can unify a variety of observations associated with the occurrence of earthquakes, some explained presently by separate frameworks and others unexplained as yet. On fault zones having mode switching activity, earthquake statistics are non-stationary on time scales shorter than several mode switching periods. This has important implications for seismic hazard assessment and other studies based on extrapolations of short duration data. The results may be relevant to other systems with many degrees of freedom and nonlinear dynamics.

2. Analysis

Fig. 1 shows a regional lithospheric model consisting of a seismogenic upper crust governed by damage rheology over a Maxwell viscoelastic substrate [13]. The model calculates the coupled evolution of earthquakes and faults in a framework incorporating damage rheology compatible with observed nonlinear and irreversible features of strain, and essential 3-D aspects of lithospheric deformation. The damage rheology, discussed in detail by Lyakhovsky et al. [27], has two types of functional coefficients: (1) a 'generalized friction coefficient' separating states associated with material degradation and healing, and (2) damage rate coefficients for positive (degradation) and negative (healing) changes. The evolving damage modifies the effective elastic properties of material in the seismogenic zone as a function of the ongoing deformation. This simulates the creation, evolution, and possible healing of fault systems in the upper brittle crust. The seismogenic zone is coupled viscoelastically to the substrate, where steady plate motion drives the lithospheric deformation. The viscous crustal deformation is calculated using variables that are vertically averaged over the crust thickness ($H + h$ in Fig. 1), while the elastic deformation is calculated with a 3-D Green function for elastic half-space. Lyakhovsky et al. [13] provide a detailed description of the simulation procedure and a large parameter-space study. Here we focus on results relevant to mode switching of seismic activity.

Fig. 2 shows map views of simulated damage in the upper crust at different times, illustrating the

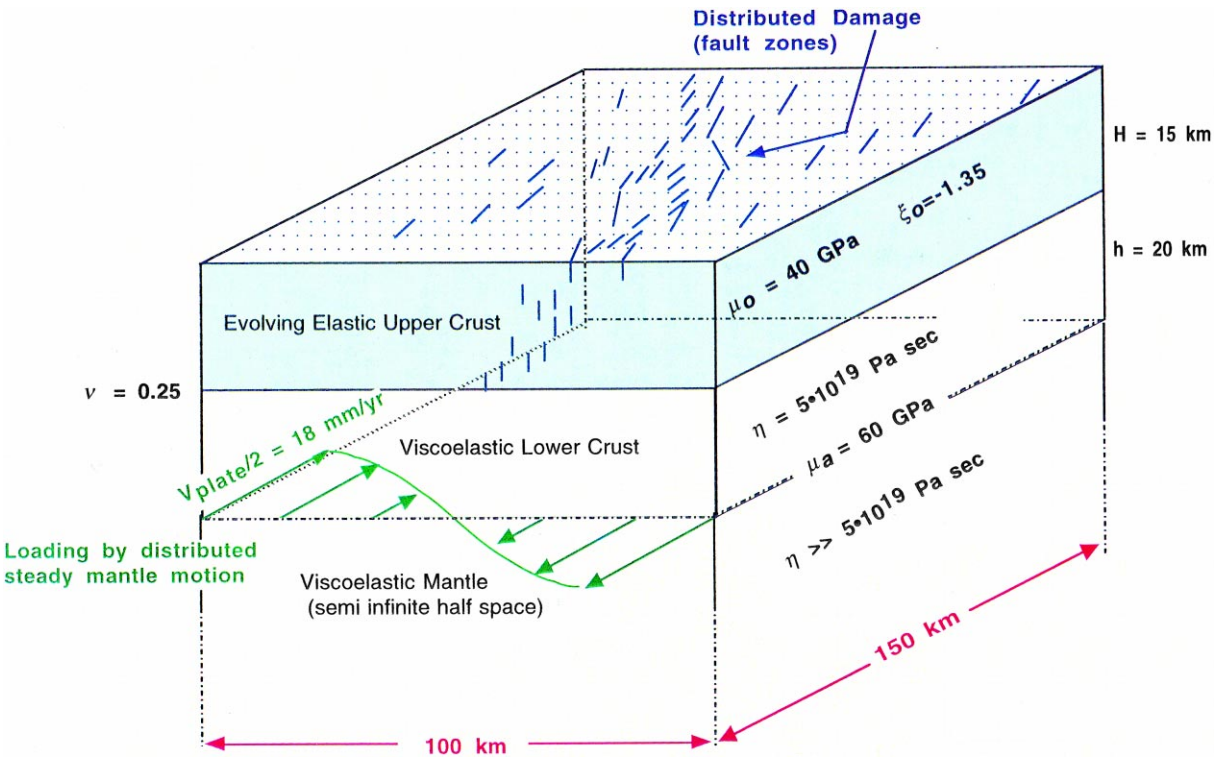

Fig. 1. Geometry and parameters for the model of ref. [13] simulating the coupled evolution of earthquakes and faults. The crust consists of a brittle seismogenic zone governed by damage rheology over a viscoelastic lower crust driven by steady mantle motion from below. H and h mark thickness of upper and lower crust layers, respectively. Parameters μ, ξ, η, and ν denote rigidity, generalized friction coefficient, viscosity, and Poisson's constant, respectively. The viscosity of the mantle is much larger than that of the lower crust. The instantaneous response of the entire model to brittle deformation in the upper crust in governed by a Green function for a 3-D elastic half-space. The boundary conditions are constant stress at the left and right edges and periodic repeats at the front and rear boundaries.

evolution of fault zones in the regional lithospheric model of Lyakhovsky et al. [13]. The boundary conditions and large-scale geometrical, rheological, and damage parameters used to generate Fig. 2 are indicated in Fig. 1 and the inset of Fig. 3. The assumed parameter values for the upper crust (thickness H, rigidity for zero damage μ_0, generalized friction coefficient ξ_0, Poisson's ratio ν), lower crust (thickness h, viscosity η, rigidity μ_a, Poisson's ratio ν), and imposed plate motion at the base of the lower crust, were determined by fitting model calculations to average observed geodetic deformation associated with the San Andreas fault in California, and additional regional constraints from observed seismological and geodetic data [13]. The key remaining parameter is the ratio of time scale for damage healing (τ_H) to time scale for loading (τ_L). Each brittle model event is associated with abrupt strength degradation and abrupt stress drop. The value of τ_H depends on the damage rate coefficients for healing and it controls the time for strength recovering after the occurrence of a brittle event. The value of τ_L depends on the boundary conditions and large-scale parameters (which determine also the average time of a large earthquake cycle) and it controls the time for reaccumulation of stress at a failed location. Relatively high ratios of τ_H/τ_L (top curve in the inset of Fig. 3) lead to the development of geometrically regular fault zones and frequency–size event statistics compatible with the characteristic earthquake distribution. Relatively low ratios of τ_H/τ_L (bottom curve in the inset of Fig. 3) lead to the development of highly disordered fault zones and frequency–size statistics compatible with the Gutenberg–Richter distribution. Lyakhovsky et al. [13] illustrate and discuss these results.

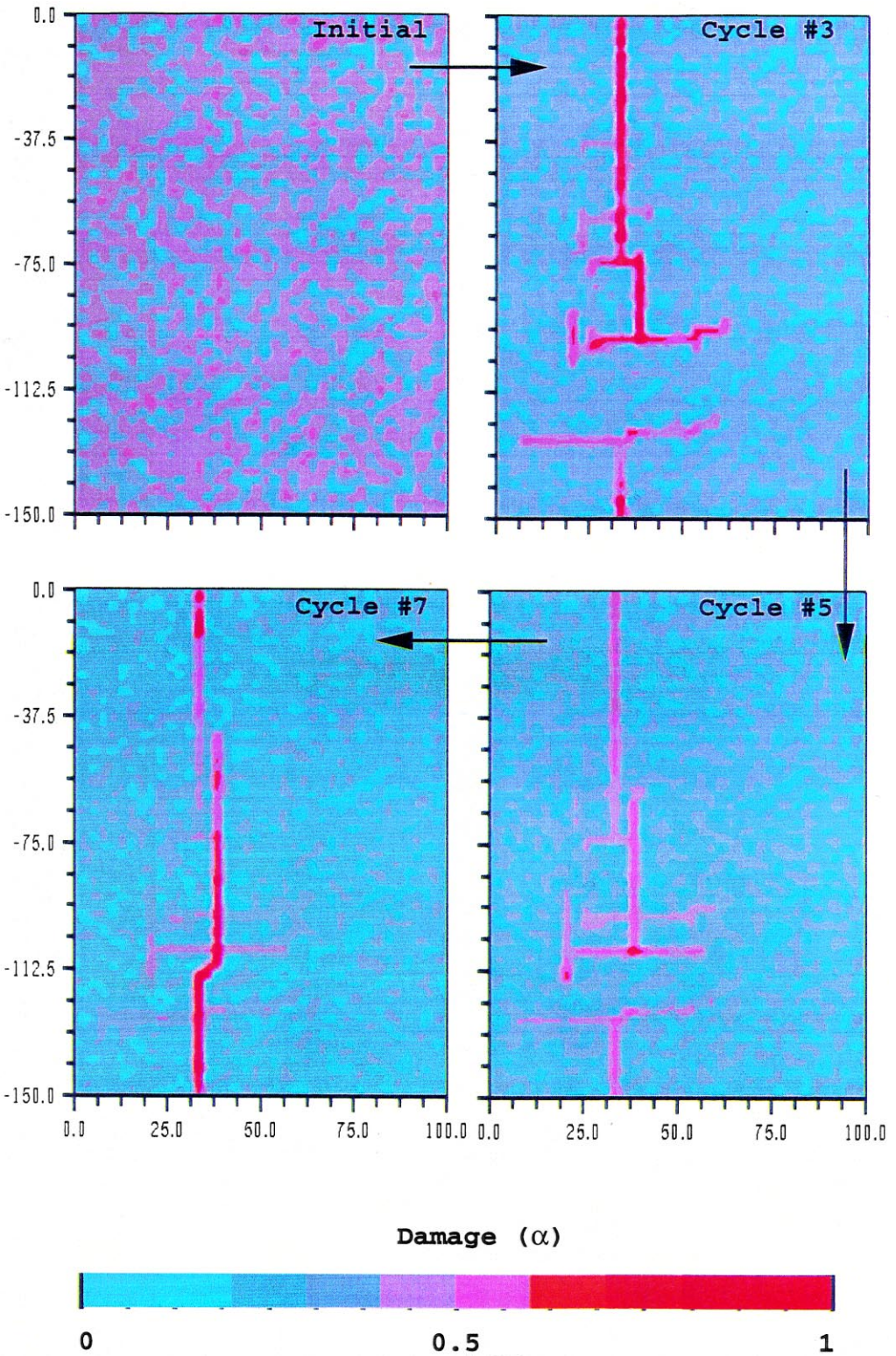
Initial
Cycle #3
Cycle #7
Cycle #5
0.0
-37.5
-75.0
-112.5
-150.0
0.0
25.0
50.0
75.0
100.0
Damage (α)
0
0.5
1

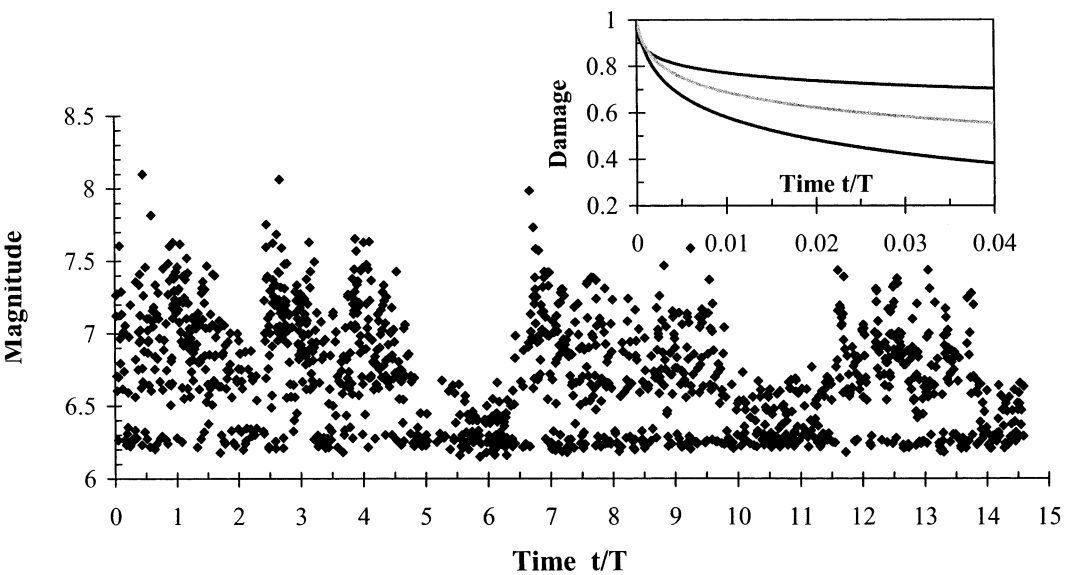

Fig. 3. A long record of model earthquakes showing mode switching of seismic response in time. The seismic activity consists of cluster periods lasting a few large earthquake cycles, separated by relatively quiet intervals of similar length. During the cluster periods, the largest possible events in the system occur, the frequency–size event statistics are compatible with the characteristic earthquake distribution, and the overall moment release is an order of magnitude higher than the inter cluster periods. In the latter intervals there are only small and intermediate-size earthquakes and the frequency–size statistics follow approximately the Gutenberg–Richter distribution. The inset shows damage evolution for different ratios of τ_H/τ_L, where τ_H is characteristic time for damage healing and τ_L is characteristic loading time. The upper line is associated with relatively high ratio of τ_H/τ_L. For such a case the damage localizes to a simple major fault zone and the frequency–size statistics follow the characteristic earthquake distribution. The bottom line is associated with relatively low ratio of τ_H/τ_L. For this case the model generates a disordered network of faults and power law frequency–size statistics. For intermediate ratios of τ_h/τ_l around the middle line, the model produces a disordered major structure as in Fig. 2 and the seismic response exhibits mode switching of activity as shown here.

The evolving fault (damage) zones of Fig. 2 and associated seismicity patterns (Fig. 3) are generated for intermediate ratios of τ_H/τ_L around the middle line in the inset of Fig. 3, small uncorrelated random noise in the spatial distribution of ξ_0, and the large-scale parameters of Fig. 1. Remarkably, for such cases the evolving fault zones maintain a level of geometrical disorder similar to those present in the last three frames of Fig. 2, and the seismic response of the model alternates between time intervals of intense seismic activity containing clusters of large events, and lower activity periods during which only small to moderate earthquakes occur (Fig. 3). The time interval of each mode of activity scales with

Fig. 2. Map views of damage distribution at four snapshots for damage healing time scale following the middle curve in the inset of Fig. 3 (where we show the associated seismic record). The model is initiated with random damage distribution peaked at about $\alpha = 0.5$. The damage does not change significantly in the first few large earthquake cycles, during which elastic strains build up and the rate of material degradation grows at locations of damage (and strain) concentration. After this transient period, at time $t/T = 3$ with T denoting average time of a large earthquake cycle, the damage localizes to a single major disordered fault zone with a large (30 km) gap and related complications in the lower part of the model. The gap is bounded by conjugate (right lateral) faults 20–30 km long. A 10 km step-over (dilatational jog) develops at the middle portion of the model. At $t/T = 5$ the gap narrows (20 km) and the overall structure is smoother. At that time the overall damage amplitude is generally lower than that of the previous panel. As shown in the related Fig. 3, this period is an intermediate interval of low seismicity between clusters of higher activity. Some high-damage zones that were previously active are healed and can hardly be recognized. At $t/T = 7$ an almost continuous disordered fault zone is established with two conjugate stepovers (dilatational and compressional). This stage represents an activation of a new cluster of high seismic activity. Further structural evolution cycles between patterns similar to those of the last three panels.

the average repeat time of large model earthquakes in the more active periods. During the low-activity intervals the rate of strain energy release in the crust is lower than the rate of energy accumulation from loading, while during the high-activity intervals the opposite is true. The model alternates between these two modes, rather than settling on a steady response with energy release rate equal the rate of energy accumulation. The frequency–size statistics of earthquakes in the intervals with and without clusters of large events are compatible approximately with the characteristic earthquake and Gutenberg–Richter distributions, respectively. The mode switching results are somewhat surprising and they may appear at first as having only a limited value associated with a curious dynamic behavior. However, as we show below, very similar behavior is seen in an independent theoretical analysis and observed earthquake and fault data.

Fig. 4 shows a model for an individual strike-slip fault system without damage evolution in a 3-D half-space [10–12,14,28]. This much simpler model contains a computational grid where evolving seismicity patterns are generated in response to ongoing loading imposed as slip boundary conditions on the other fault regions. The brittle properties of the computational grid are characterized by static strength threshold and arrest stress distributions that are spatially heterogeneous but fixed in time, and a dynamic weakening coefficient ε. The latter simulates a reduction from static friction to dynamic strength at a point on a fault sustaining multiple slip episodes during a given model earthquake [10]. The stress transfer along the fault due to the imposed boundary conditions and failure episodes in the computational grid is calculated with a 'mean field' Green function [28,14] that replaces the actual elastic stress response to dislocations [10–12] with a constant value. The mean-field Green function can not be used to calculate details of deformation fields or other specific phenomena, but it provides an appropriate tool for studying questions such as possible types and exponents of statistics characterizing event populations generated under different conditions [29].

Dahmen et al. [14] mapped the dynamics of this fault system onto a phase diagram (Fig. 5a) spanned by the dynamic weakening coefficient ε and a conservation parameter c related to dissipation of stress

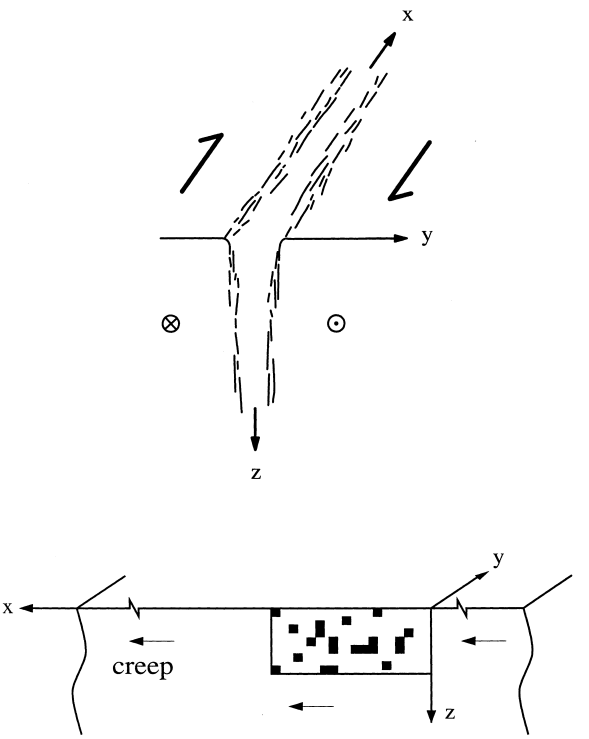

Fig. 4. (Top) A schematic representation of an individual strike-slip fault system with a 3-D geometric disorder. (Bottom) A simple representation of the 3-D disordered fault system by a 2-D fault embedded in a 3-D half-space. Each fault location $(x, y = 0, z)$ represents deformation in a volume centered on the line (x, y, z). The geometric disorder is modeled as disorder in strength properties of the planar fault. The rectangular section is a computational grid where black and white patches denote locations of relatively high and relatively low stress thresholds to failure. The other fault regions creep at constant velocity. (Modified from [12].)

transfer and the size of the system. The values of ε range from 0 at no weakening (dynamic friction equals static friction) to 1 at complete weakening (dynamic friction equal 0). The values of c range from 0 at complete dissipation (corresponding here to the unphysical case of a fault that is loaded, in addition to the boundary conditions on the continuation of the computational grid, directly at the rupture zone) to 1 at complete conservation of stress transfer (corresponding to the physical case of a fault loaded by motion of tectonic plates far away and deformation of the surrounding material). At exactly $\varepsilon = 0$ and $c = 1$ there is a critical point of a second-order phase transition [28] and the frequency–

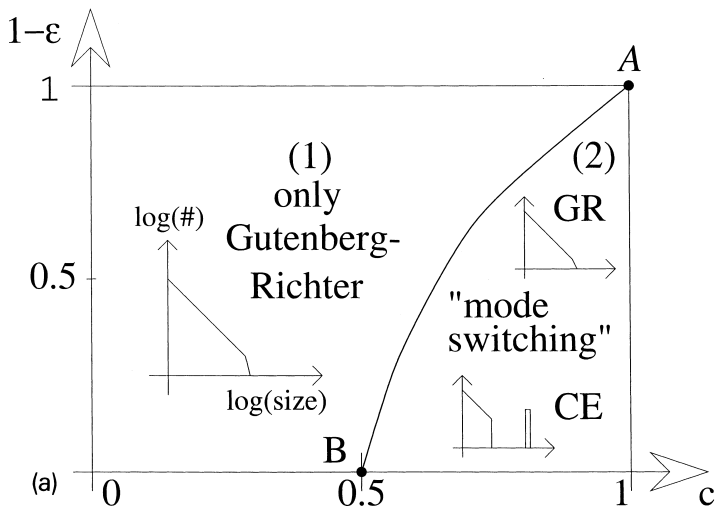

Fig. 5. (a) Phase diagram of simulated frequency–size earthquake statistics as a function of conservation of stress transfer c and dynamic weakening coefficient ε. A value $c = 1$ corresponds to a fault loaded from a 'far-field' edge of a large spatial domain with no loss of stress transfer, whereas $c < 1$ corresponds to loading from the edge of a small spatial domain or the existence of a loss mechanism. A value $\varepsilon = 0$ corresponds to static friction only, whereas $\varepsilon > 0$ corresponds to the existence of both static and kinetic friction levels. Models with parameter values in region 1 can only produce Gutenberg–Richter (GR) types of statistics. Models in the more realistic region 2 can produce both Gutenberg–Richter and characteristic earthquake (CE) types of statistics. In such cases, a finite fault will produce one type of statistics for a certain persistence time and then spontaneously switch to another mode in which it produces the other type. (Modified from [14].)

size distribution of simulated model earthquakes is given by the Gutenberg–Richter power law relation. If ε and c belong to region 1 of the phase diagram, the frequency–size statistics consist of a truncated power law, a form generally compatible with the Gutenberg–Richter distribution. Remarkably, we find also here that for a range of dynamic weakening and dissipation parameters that map into the more physical region 2, the seismicity (Fig. 5b, top) switches spontaneously back and forth, as in the model of Lyakhovsky et al. [13], between time periods containing large events following the characteristic earthquake distribution, and time periods containing only small to moderate earthquakes following a truncated power law distribution.

As discussed by Dahmen et al. [14], the activity switching in this model results from episodic global reorganization of the mode of strain energy release of the fault system, reflected in the configurational entropy of stress states on the fault (Fig. 5b, bottom). This is associated with a statistical competition between a tendency for a synchronized behavior leading to clusters of large earthquakes and the characteristic earthquake distribution, and a tendency for disordered response leading to Gutenberg–Richter type statistics without a preferred event size. For model parameters in region 2 of Fig. 5a, these two opposite tendencies are roughly equal in strength. A similar dynamic mechanism probably generates the alternating 'undershoot' and 'overshoot' responses in the regional model of Lyakhovsky et al. [13].

3. Discussion

We study long histories of simulated seismicity patterns using two separate frameworks. The first, more realistic model [13], employs a lithospheric domain with a regional seismogenic zone governed by damage rheology, viscoelastic substrate, multiple evolving faults, and 3-D elastic Green function for stress transfer due to brittle failures. The second, simpler model [14], simulates seismicity on a single fault system with prescribed planar geometry, elementary rheology, and a mean field approximation of the stress transfer function. The more realistic framework can address a much broader class of questions than the simpler model can. However, this

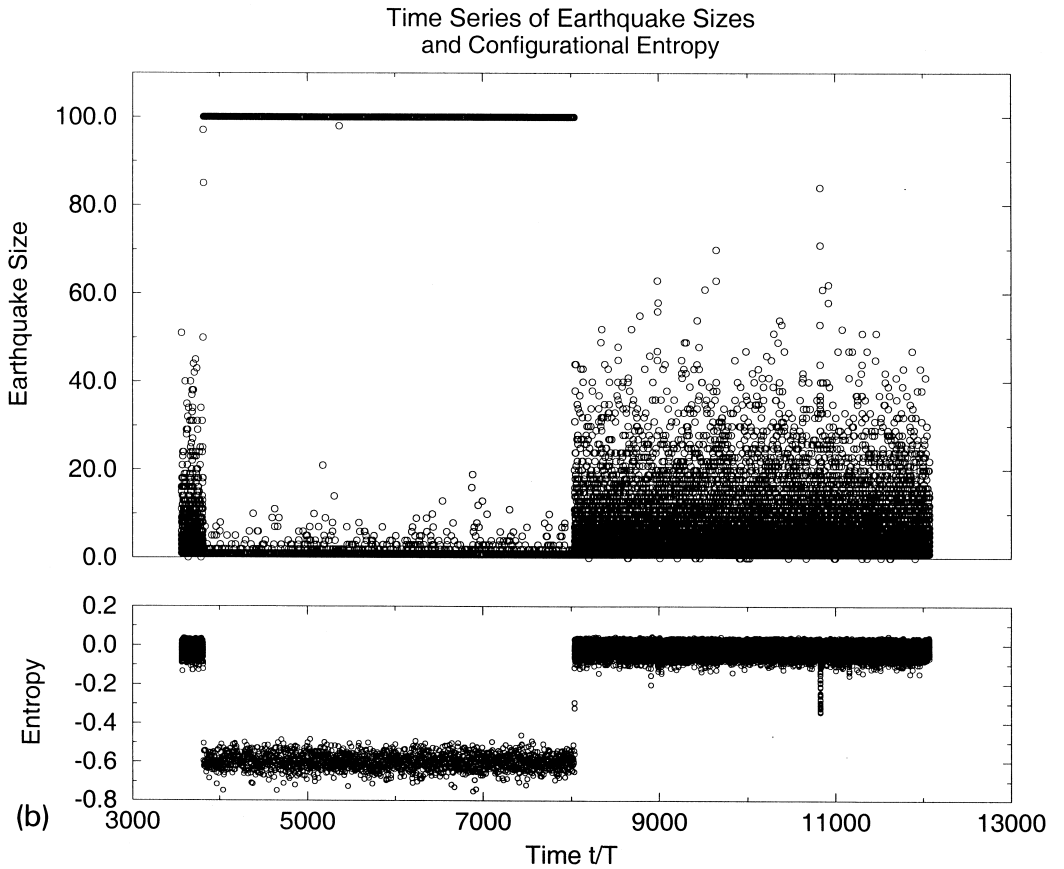

Fig. 5 (continued). (b) Sample time series of earthquake sizes (top) and corresponding configurational entropy (bottom). The model time t is given in units of the average repeat time T of the largest earthquakes in the characteristic earthquake phase. The earthquake size is given in units of rupture area. The top panel shows that after switching at $t/T \approx 3800$ from the Gutenberg–Richter phase with mostly small earthquakes to the characteristic earthquake phase with quasi-periodically recurring large earthquakes and only very small earthquakes in between, the fault remains in the characteristic earthquake phase for roughly 4200 T before it spontaneously switches back into the Gutenberg–Richter phase. The configurational entropy is defined as the entropy of the distribution of stresses along the fault and is computed as a function of time. Large entropy implies large variations of stress states on the fault. Such stress states produce Gutenberg–Richter type of statistics. Small entropy indicates synchronization and a narrow distribution of stress states. In this case all parts of the fault tend to rupture together in one large event, in which they simultaneously release their stresses. Subsequently, different parts of the fault get reloaded more-or-less simultaneously (while producing only very few small earthquakes), until another large earthquake relaxes the entire fault and the cycle is repeated, thereby producing characteristic earthquake type of statistics. (Modified from [14].)

is somewhat compensated by a greater ability of the simpler model to obtain a basic understanding of common underlying dynamic mechanisms. In both cases, we find that the models generate for ranges of parameters self-driven mode switching of seismic activity. The actual mode switching times are statistical events and the average persistence time for each mode, in the more realistic model [13], is on the order of a few large earthquake cycles. Examples of large earthquake cycles on major natural active fault zones are hundreds of years for the San Andreas fault and thousands of years for the Dead Sea transform in Israel. Thus, observational confirmation of response switching on large fault systems of the type predicted by our models requires data sets that are many thousands of years long.

Marco et al. [15] compiled from slip and damage events in sediments of the Lisan Lake in the Dead

Sea region, Israel, a 50 kyr history of moderate and large ($M \geq 6$) earthquakes occurring along the Dead Sea transform in that area. Their obtained paleoseismic data consist of alternating time intervals, on the order of 5–10 kyr each (i.e., a few large earthquake cycles), with distinctly different seismic character. In half of the intervals the sedimentary record contains clear signatures of moderate to large events, while in the other half very few or no such signatures exist. Leonard et al. [16] performed a Bayesian statistical analysis of 50 kyr long paleoseismic earthquakes along the Arava segment of the Dead Sea transform, approximately 100 km south of the study area of ref. [15]. The data sets of [15,16] overlap only partially in time and span together about 70 kyr. Leonard et al. [16] concluded that there was a clear change in the seismic behavior of the Arava fault around 15 kyr ago. In the interval of 15–35 kyr ago (a period overlapping with the most recent cluster of intense seismic activity in the data of Marco et al. [15]), the statistical analysis of earthquakes on the Arava fault favors the characteristic earthquake distribution. In contrast, the frequency–size statistics of earthquakes occurring on that fault in the last 15 kyr are compatible with either the Gutenberg–Richter distribution or a characteristic earthquake distribution with a smaller characteristic earthquake magnitude. Ambraseys and others [17–19] assembled long earthquake histories for the North and East Anatolian faults in Turkey and other faults in the Middle East. Their compiled earthquake histories show, like the Dead Sea transform, alternating periods of activity with and without moderate to large earthquakes. There is recent evidence for similar mode switching on the Altyn Tagh fault in China [20]. These fluctuations of earthquake activity, which until now were unexplained, appear to reflect mode switching of the seismic response of individual large fault systems, as seen in our model calculations. It is difficult to explain these observations by other mechanisms, such as interaction with near-by large faults, since the Dead Sea transform, North Anatolian, East Anatolian, and Altyn Tagh faults are each the only major fault system in the associated tectonic domain.

Other data sets are also compatible with the mode switching of seismic activity discussed in this work. These include episodic clusters of large historic earthquakes in the Middle East [23] and east Asia [24], evidence for several widely separated periods with and without large earthquakes in the new Madrid, eastern US, seismic zone [22], changes in the character of activity along several faults in the Basin and Range, western US, province [25], episodic clustering of activity in the last 10 kyr along fault segments in the rupture zone of the 1992 Landers, CA, earthquake [21], and geologic data combined with recent geodetic and seismological measurements showing changes in the character of accumulation and release of seismic energy on the San Miguel fault, Mexico [26]. Some of the latter observations may result from other physical mechanisms or incompleteness of data. However, such explanations can not hold for all the discussed data, especially those associated with the Dead Sea transform, North Anatolian, East Anatolian, and Altyn Tagh faults.

An extreme manifestation of mode switching of seismic activity may produce transitions between brittle (seismic) and effectively creeping (or aseismic) responses to tectonic loading. It is interesting to speculate that the currently creeping segment of the central San Andreas fault had in the past (and may have in the future) large earthquake ruptures. If so, paleoseismic trenching may provide evidence for past large earthquakes in the creeping segment, and seismological, geodetic, and other imaging methods may show signatures of locked fault zone structures. We note that Eberhart-Phillips and Michael [30] pointed out, based on seismic tomography of the central San Andreas fault, that the velocity structure along part of the creeping segment is similar to that of the locked section associated with the rupture zone of the great 1857 earthquake.

4. Conclusions

The debate on the form of frequency–size statistics of earthquakes has been polarized so far [4–12] into either the Gutenberg–Richter or characteristic earthquake distributions but not both. The theoretical and observational results discussed in this paper indicate that the seismic behavior of a fault system can change spontaneously from response following one type of statistics to the other. In places where such mode switching occurs, the time scale over which

the seismicity may be regarded as stationary is at least several times larger than the persistence time in each mode, e.g. 5–10 kyr for the San Andreas fault and 50–100 kyr for the Dead Sea transform. These results have far reaching implications for the overall understanding of earthquake and fault dynamics, and various specific applications such as seismic hazard assessment. We note that fluctuations similar to our mode switching results may be present in the behavior of other systems with many degrees of freedom and nonlinear dynamics, such as communication networks [31], climate [32], and the Earth magnetic field [33].

Acknowledgements

We thank Geoff King, Andy Michael, Phil Pollett, and Rick O'Connell for useful comments. The research was supported by the National Science Foundation (grant EAR-9725358) and the Southern California Earthquake Center (based on NSF Cooperative Agreement EAR-8920136 and USGS Cooperative Agreement 14-08-0001-A0899). ***[RC]***

References

[1] D.W. Simpson, P.G. Richards (Eds.), Earthquake prediction, American Geophysical Union, Washington, DC, 1981, 680 pp.
[2] Y. Utsu, Y. Ogata, R.S. Matsu'uara, The centenary of the Omori formula for a decay law of aftershock activity, J. Phys. Earth 43 (1995) 1–33.
[3] Y.Y. Kagan, Observational evidence for earthquakes as a nonlinear dynamic process, Physica D 77 (1994) 160–192.
[4] Y.Y. Kagan, Comment on 'The Gutenberg–Richter or characteristic earthquake distribution, which is it?' by Wesnousky (1994), Bull. Seismol. Soc. Am. 86 (1996) 274–285.
[5] Y.Y. Kagan, Seismic moment–frequency relation for shallow earthquakes: Regional comparison, J. Geophys. Res. 102 (1997) 2835–2852.
[6] S.G. Wesnousky, The Gutenberg–Richter or characteristic earthquake distribution, which is it?, Bull. Seismol. Soc. Am. 84 (1994) 1940–1959.
[7] S.G. Wesnousky, Reply to comment by Kagan [4], Bull. Seismol. Soc. Am. 86 (1996) 285–291.
[8] M.W. Stirling, S.G. Wesnousky, K. Shimazaki, Fault trace complexity, cumulative slip, and the shape of the magnitude–frequency distribution for strike-slip faults: a global survey, Geophys. J. Int. 124 (1996) 833–868.
[9] D.P. Schwartz, K.J. Coppersmith, Fault behavior and characteristic earthquakes: examples from the Wasatch and San Andreas fault zones, J. Geophys. Res. 89 (1984) 5681–5698.
[10] Y. Ben-Zion, J.R. Rice, Earthquake failure sequences along a cellular fault zone in a 3D elastic solid containing asperity and nonasperity regions, J. Geophys. Res. 98 (1993) 14109–14131.
[11] Y. Ben-Zion, J.R. Rice, Slip patterns and earthquake populations along different classes of faults in elastic solids, J. Geophys. Res. 100 (1995) 12959–12983.
[12] Y. Ben-Zion, Stress, slip and earthquakes in models of complex single-fault systems incorporating brittle and creep deformations, J. Geophys. Res. 101 (1996) 5677–5706.
[13] V. Lyakhovsky, Y. Ben-Zion, A. Agnon, Earthquake cycle, fault zones and seismicity patterns in a rheologically layered lithosphere, J. Geophys. Res. (1999) (submitted).
[14] K. Dahmen, D. Ertas, Y. Ben-Zion, Gutenberg Richter and characteristic earthquake behavior in simple mean-field models of heterogeneous faults, Phys. Rev. E 58 (1998) 1494–1501.
[15] S. Marco, M. Stein, A. Agnon, H. Ron, Long term earthquake clustering: a 50,000 year paleoseismic record in the Dead Sea graben, J. Geophys. Res. 101 (1996) 6179–6192.
[16] G. Leonard, D.M. Steinberg, N. Rabinowitz, An indication of time-dependent seismic behavior — an assessment of paleoseismic evidence from the Arava fault, Israel, Bull. Seismol. Soc. Am. 88 (1998) 767–776.
[17] N. Ambraseys, C. Finkel, The Seismicity of Turkey, Eren Press, Istanbul, 1995, 240 pp.
[18] N. Ambraseys, C. Melville, A History of Persian Earthquakes, Cambridge University Press, London, 1982.
[19] N. Ambraseys, C. Melville, R. Adams, Seismicity of Egypt, Arabia and the Red Sea, Cambridge University Press, London, 1994.
[20] G. King, pers. commun., 1998.
[21] T.K. Rockwell, S. Lindvall, M. Herzberg, D. Murbach, T. Dawson, G. Berger, Paleoseismology of the Johnson Valley, Kickcapoo and Homestead Valley faults of the Eastern California Shear Zone, Bull. Seismol. Soc. Am. (1999) (in review).
[22] J.L. Sexton, P.B. Jones, Evidence for recurrent faulting in the New Madrid seismic zone, Geophysics 31 (1986) 1760–1788.
[23] A. Nur, E.H. Cline, Plate tectonics, earthquake storms, and system collapse at the end of the late bronze age in the Aegean and eastern Mediterranean, J. Archaeol. Sci. (1999) (in press).
[24] J.B. Kyung, K. Oike, T. Hori, Temporal variations in seismic and volcanic activity and relationship with stress field in east Asia, Tectonophysics 267 (1996) 331–342.
[25] R.E. Wallace, Grouping and migration of surface faulting and variations in slip rates on faults in the great basin province, Bull. Seismol. Soc. Am. 77 (1987) 868–876.
[26] C.K. Hirabayashi, T.K. Rockwell, S.G. Wesnousky, M.W. Stirling, F. Suarez-Vidal, A neotectonic study of the San

Miguel–Vallecitos Fault, Baja California, Mexico, Bull. Seismol. Soc. Am. 86 (1996) 1770–1783.
[27] V. Lyakhovsky, Y. Ben-Zion, A. Agnon, Distributed damage, faulting, and friction, J. Geophys. Res. 102 (1997) 27635–27649.
[28] D.S. Fisher, K. Dahmen, S. Ramanathan, Y. Ben-Zion, Statistics of earthquakes in simple models of heterogeneous faults, Phys. Rev. Lett. 78 (1997) 4885–4888.
[29] Ma, S.K., Modern Theory of Critical Phenomena, Benjamin (1976).
[30] D. Eberhart-Phillips, A.J. Michael, Three-dimensional velocity structure and seismicity in the Parkfield region, central California, J. Geophys. Res. 98 (1993) 15737–15758.
[31] R.J. Gibbens, P.J. Hunt, F.P. Kelly, Bistability in communication networks, in: G.R. Grimmett, D.J.A. Welsh (Eds.), Disorder in Physical Systems, Oxford University Press, Oxford, 1990, pp. 113–127.
[32] C. Appenzeller, T.F. Stocker, M. Anklin, North Atlantic oscillation dynamics recorded in Greenland ice cores, Nature 283 (1998) 446–449.
[33] S.P. Lund, G. Acton, B. Clement, M., Hastdt, M. Okada, T. Williams and others, Geomagnetic field excursions occurred often during the last million years, Eos 79 (1998) 178–179.